AN INTEGRATED ROBOTIC WORK CELL FOR HIGHLY AUTOMATED ULTRASONIC INSPECTION OF COMPLEX CFRP PARTS

Klaus Schlachter[1], Sebastian Zambal[1], Christian Eitzinger[1],
Andrey Bulavinov[2], Roman Pinchuk[2]

[1] PROFACTOR GmbH
Im Stadtgut A2
4407 Steyr

[2] ACS-Solutions GmbH
Science Park 2
66123 Saarbrücken

ABSTRACT

Ultrasonic inspection of complex structural parts made of carbon fibre reinforced plastic (CFRP) typically includes a set of tedious time-consuming manual tasks. The data acquisition process is difficult to adapt to varying geometries of specimens and different test equipment. Furthermore, automatic data evaluation is challenging. In order to increase the degree of automation for robot-based ultrasonic inspection, a set of practical problems needs to be addressed: automatic part localization, inspection path planning, robot motion generation, fast data processing, and automatic defect detection and classification. We introduce an integrated workflow that copes with the above challenges. We present a highly automated robotic work cell for ultrasonic inspection. Results and limits of the system are discussed for a set of challenging sample parts.

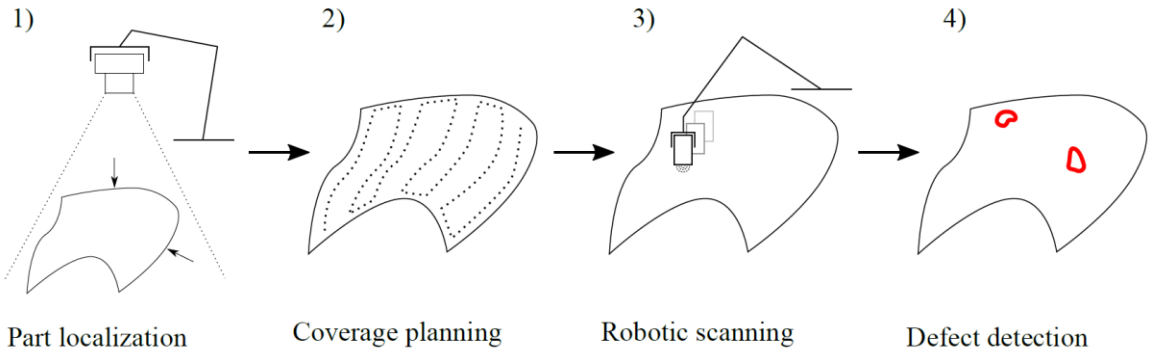

Figure 1: Overview about the workflow of robotic ultrasonic inspection presented in this paper: 1) vision system for part localization, 2) coverage path planning, 3) data acquisition, and 4) defect detection.

1. INTRODUCTION

Progress in production processes enables the realization of structural carbon fibre reinforced polymer (CFRP) parts with more and more complex geometries. Usage of safety-critical CFRP parts requires a seamless inspection of each individual product [1]. Conventional ultrasonic testing involves time consuming manual tasks in order to gather ultrasonic data. Further, domain experts typically evaluate the gathered ultrasonic data manually. Thus, inspection results highly depend on the judgment of the inspector. Therefore, automation has not only the potential of enormous time and cost savings, but can also reduce the variation of results. In the scope of the project SonicScan[1] we are developing methods for immersion testing with an articulated industrial robot. The focus is thereby put on the automation of the complete

[1] http://sonicscan.eu

inspection process. Figure 1 shows the main steps in the proposed workflow: part localization, coverage planning, robotic scanning, and defect detection.

Coverage planning refers to the determination of a robot path, which covers a surface or volume of interest without collisions. This problem needs to be solved for a wide variety of robotic systems, for example cleaning or demining robots. A common approach for this type of systems is to split the surface into cells, which can be covered by meander-shaped paths [2]. However, improvement of the state of the art is still required since conventional methods typically only address planar surfaces, which are not directly portable to inspection problems regarding industrial robots. Our approach builds upon this idea of subdividing a complex surface into smaller cells that can be handled more easily.

Coverage planning for more complex two-dimensional surfaces embedded in the three-dimensional space is for example addressed in the motion planning of underwater structure inspection, painting and bush trimming robots [2, 3, 4]. Ultrasonic scanning requires to move the sensor along a path which maintains a specific distance to the surface. An existing approach is based upon generating an offset surface, i.e. a surface with a defined and constant distance to the target surface [4]. This allows to apply conventional algorithms on that virtual surface. In our method, we deploy a process model which contains the requirements for relative placement with respect to the part surface (distance, angle).

Over the past years, impressive classification performance of deep convolutional neural networks has been demonstrated for a number of hard computer vision problems (ImageNet, PASCAL Visual Object Classes). We aim at making use of these methods for quality control based on ultrasound measurements. An elegant neural network architecture, which was originally proposed for segmentation of 2-dimensional histological images, is the so called U-Net [5]. It consists of a set of encoding layers followed by a set of decoding layers. Additional direct connections from encoding layers to decoding layers of equal spatial resolution support the efficient use of local features in combination with global context information. By replacing 2D convolutions with 3D convolutions, the original U-Net architecture can be modified so that it accepts volume data as input. This 3D version of the U-Net outputs volumetric segmentation masks. Here, we apply the U-Net architecture to ultrasonic inspection data.

This paper is organized according to figure 1. In section 2 we outline a vision system for localizing the part to be inspected inside the work space of the robot. In section 3 we present an algorithm for automatic planning of the robot motion that is needed to acquire ultrasonic inspection data. In section 4 we briefly outline our approach for synchronization of robot motion and ultrasound signal acquisition using time stamps. A method for automatic analysis of volumetric ultrasound data is outlined in section 5 and conclusions and future work are provided in section 6.

2. AUTOMATIC PART LOCALIZATION

A very basic step for doing robot-based inspection is to localize the part within the workspace of the robot. In simple scenarios, this is done manually using a measurement tip on the robot. When different parts are to be inspected or the position of parts changes frequently, manual calibration can become very time-consuming and tedious. In the workflow that we consider here, the part to be inspected is not fixed within the workspace. It is simply placed inside a water basin on a supporting table. The great advantage is that no underwater fixture mechanism is required and the process of inserting the part into the workcell can either be done manually or automatically (e.g. by the inspection robot equipped with a tool-changer). This can be done

without taking much care of the accurate positioning of the part. Exact localization is done in a separate step as outlined in the following.

We propose the use of a stereo vision setup. The advantage of such a system is that it works contact-less and can be implemented with low costs for hardware. Basically, only a camera together with image processing software is required. The single camera is mounted on the inspection robot and images of the workspace are taken at different robot positions. Individual points on the surface of the inspected parts are then localized via triangulation. An important difference to standard stereo vision systems is that refraction needs to be taken into account. We follow an approach based on explicit modeling of the refraction of light rays [6].

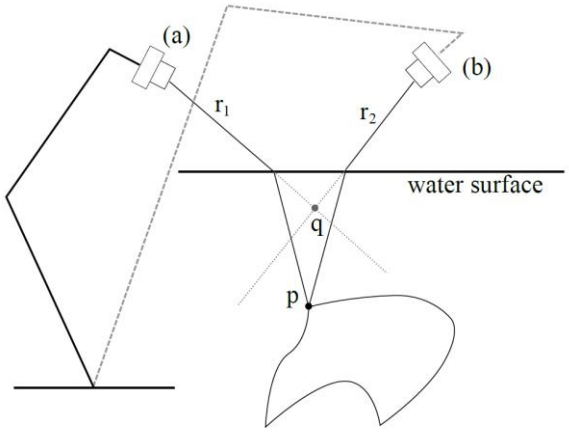

Figure 2: Stereo vision for under-water object localization. See text for details.

Figure 2 illustrates how 3D points are triangulated using the proposed method. The robot moves the camera to different positions (e.g. positions (a) and (b). An image is taken at each of these positions. Unique points on the part surface are identified in the stereo images. According to the calibration parameters of the camera, view rays are calculated (r_1 and r_2). However, their intersection provides a wrong position q. Refraction needs to be taken into account to get the correct position p of a point on the part. With at least three points on the part surface it is then possible to calculate the correct alignment of part coordinate frame and robot work space.

3. COVERAGE AND PATH PLANNING

For coverage and path planning, we propose the usage of a process model, which maps a surface point to a sensor position and orientation. Dependent on the local thickness of the specimen, the sensor needs to be positioned in a certain distance to the surface. In addition, to obtain an ideal sound coupling, the wave vector needs to be perpendicular to the specimen's surface. The rotation about the surface normal has no impact on the inspection process and is used as a degree of freedom for path planning. The following section addresses the problem of finding a path that meets these requirements. We assume that each inspection position needs to be passed exactly once.

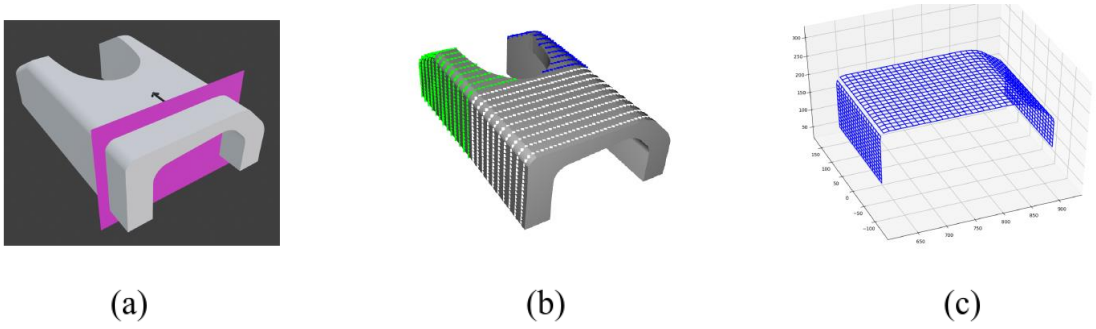

(a) (b) (c)

Figure 3: A slicing plane sweeps over the specimen (a). At locations where the connectivity changes, additional cells are introduced leading to three cells in (b). In (c) the graph representing the white cell from (b) together with their connectivity is shown. Connections (edges) between vertices exist if their spatial distance and local curvature is small.

Hereinafter, path planning consists of three steps: (i) the surface is segmented into connected regions, which – without regarding collision avoidance – can be captured with meander-shaped movements, (ii) valid paths in the robot's joint space are calculated and (iii) the order of individual segments is optimized by finding a solution to the associated traveling salesman problem.

3.1 Segmentation

As a starting point, we use a cellular decomposition [2], which allows the decomposition of the specimen's surface into cells, which can be covered individually by meander-shaped Cartesian paths. These Cartesian paths are generated by sweeping a slicing plane over the specimen. At points where the connectivity changes (e.g. forking), the surface is split into new cells (see Figure 3(a) and (b)).

Ideally, inspected points should be spatially close to each other, whereas the sensor orientations should be similar in order to keep joint movements small. We construct an undirected graph consisting of vertices $(\boldsymbol{p}, \boldsymbol{n})$ with the position $\boldsymbol{p}$ and the sensor orientation $\boldsymbol{n}$. An edge e_{ij} connects two vertices K_i and K_j, if the distance and the inner product of the sensor orientations are below certain -to be defined -parameters $d_{\max}$ and $c_{\max}$ (similar to [7], see Fig. 3(c)):

$$e_{ij} = ||\boldsymbol{p}_i - \boldsymbol{p}_j|| < d_{max} \wedge \langle \boldsymbol{n}_i, \boldsymbol{n}_j \rangle < c_{max}. \quad (1)$$

For the resulting segments formed by connected vertices, we plan paths by utilizing the method described in the following subchapter.

3.2 Path Planning

Path planning is considered for non-redundant six-axis industrial robots with the most common architecture consisting of a trunk, shoulder, upper arm, forearm, and wrist. Regular end-effector poses of these robots have eight unique inverse kinematics (IK) solutions due to three joint singularities. The IK solutions can be grouped by their appearance in the joint space (e.g. shoulder right, wrist down, elbow up) referred to as manipulator poses (MP). Moving the robot from one MP to another generally requires large joint motions and therefore should be avoided. The presented method generates inspection paths, which allow for inspection of segments with minimal re-orientations.

3.2.1 Problem definition

The vertex inspection order is predefined by the meander-shaped Cartesian path. Moving from one k-th inspection position to the next, ideally causes small robot motions in the configuration space. We denote the rotation about the sensor axis at individual positions as φ_k.

The rotation about the sensor axis between two consecutive vertices needs to be limited. In order to find a solution, the following control problem is defined:

$$\begin{aligned} & \varphi_{k+1} = \varphi_k + u_k, \quad k = 0 \dots N-1 \\ \text{s.t.} \quad & c(k, \varphi_k) = 0 \\ & u_k \in [-u^{max}, u^{max}] \end{aligned} \tag{2}$$

with the control input u_k and its box constraints specifying the maximal accepted rotation angle about the sensor axis between consecutive vertices, the path constraint $c \rightarrow \{0,1\}$ mapping to zero if the configuration does not cause any collisions, and the number of vertices N.

3.2.2 Path construction

To find a solution, firstly a map $m : k \times \varphi \rightarrow \{0,1\}$ with the discrete angles $\varphi \in \{0, u^{max}, 2u^{max}, \dots, 2\pi\}$ is generated, which subsequently allows an easy construction of a valid path backwards from $k = N - 1$ to $k = 0$:

- For $k = 0$, the value is set equal to the value of the collision detection $m(0, \varphi) = c(0, \varphi)$.
- For $k \neq 0$, the value is set to 0 if $c(k, \varphi) = 0$ and an angle $\varphi_{k-1} \in \{\varphi - \underline{u}^{max}, 0, \varphi + u^{max}\}$ exists such that $m(k-1, \varphi_{k-1}) = 0$. That means that pairs (k, φ) only map to zero if they represent collision free configurations and allow to reach a valid point at time $k-1$ in compliance with the box constraints of the input variable.

For every valid terminal point $(N-1, \varphi_{N-1})$, i.e. $m(N-1, \varphi_{N-1}) = 0$, finally a unique bang-bang solution can be found by constructing it backwards in time:

$$u_k = \begin{cases} 0 & \text{if } m(k, \varphi_{k+1}) = 0 \\ \text{otherwise} & u^{max}, \text{ if } m(k, \varphi_{k+1} - u^{max}) = 0 \\ & -u^{max}, \text{ if } m(k, \varphi_{k+1} + u^{max}) = 0 \end{cases} \tag{3}$$

Fig. 4 shows the resulting map and the backwards construction of the path for the right segment of Fig. 3(c).

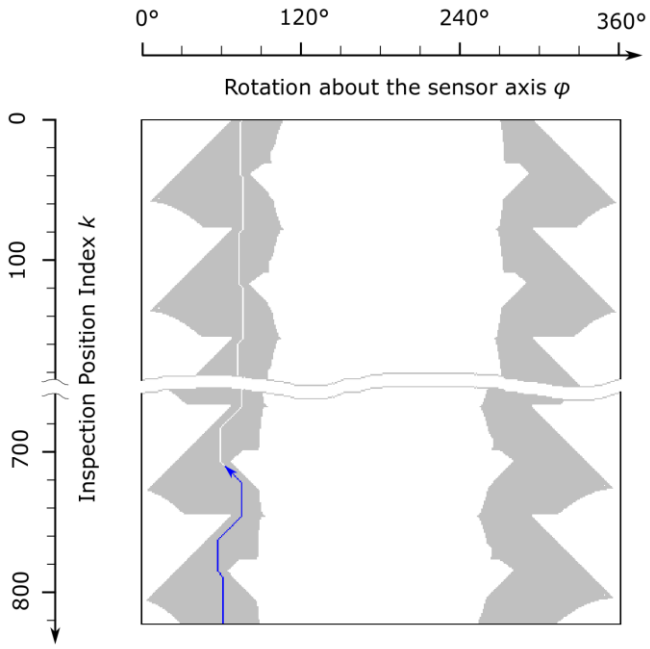

Figure 4: Regions where $m(k; \varphi) = 0$ are encoded gray. Within that region, we search for a valid path. The backwards construction of the path is indicated as a blue arrow.

3.3 Inspection Plan

In order to plan motions between segments, collision free paths are generated using the RRT implementation of OMPL [8]. The traveling salesman problem associated with finding an optimal inspection order of individual regions is solved with a simulated annealing solver using an objective function that assesses the path length in the joint space.

4. ROBOTIC SCANNING

Ultrasonic scanning is done along with the robot moving the ultrasound head according to the previously calculated inspection path. In order to assign the correct positions to individual ultrasound signal captures, robot motion and ultrasound signal acquisition need to be synchronized. We deploy an approach based on time stamps. Each robot position and ultrasound capture is assigned a time stamp from different hardware clocks, i.e. robot controller clock and ultrasound acquisition device. Via synchronization of both clocks, the correct assignment of positions to ultrasound captures is possible.

Recorded ultrasound echoes are integrated into a volumetric reconstruction of the inspected part. This dense volume representation is the basis for further processing of the data for defect detection.

5. DEFECT DETECTION

We aim at automatic detection and classification of defects within volumetric ultrasound data. This is the last step in the complete inspection workflow. Specifically, we aim for segmentation of interesting regions and the assignment of class labels to these regions. We propose the use of a deep neural network to achieve this. Our approach builds upon the neural network architecture proposed recently for segmentation of medical volume data [9]. This architecture can be modified easily to support practically any number of output classes that are suitable for the respective application.

When using machine learning, it is often difficult to acquire a sufficient amount of training data. We tackle this issue by using artificially generated data. To demonstrate the performance of our network, we implemented the following classes: "background", "cuboid", and "cylinder". We implemented a randomized process that generates volume data randomly containing cuboids and cylinders. In order to make it difficult for the neural network to learn these shapes, random noise was added.

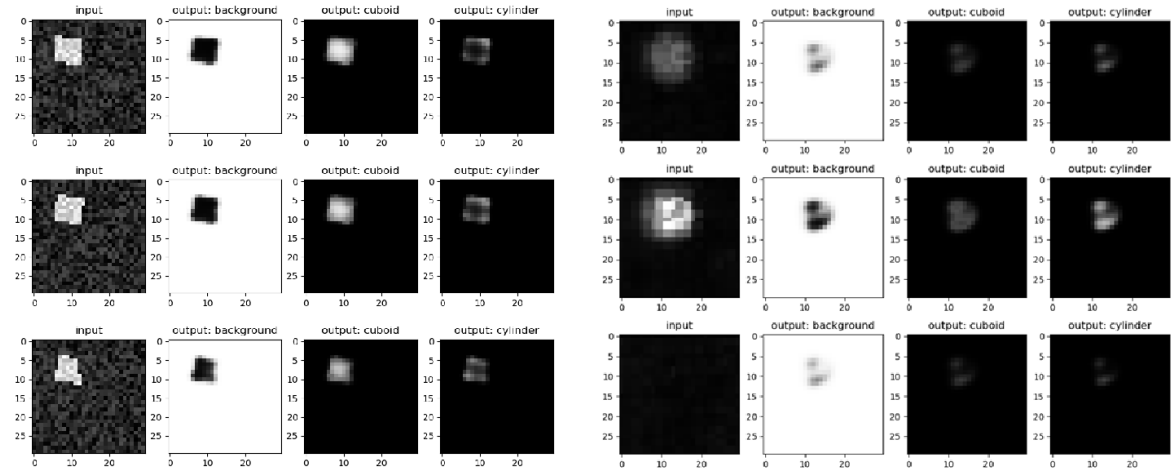

Figure 5: Application of the neural network to artificial data (a) and real ultrasonic scan data (b). Both, (a) and (b) show 4 columns that represent neural network input (left column) and neural network output for classes "background", "cuboid", and "cylinder" (remaining columns).

Figure 5 shows the output of the network for artificial data that includes a cuboid (a) and real data with a cylindrical hole (b). Rows in Figure 5 represent individual slices of the volumes. The columns show the input to the neural network and output maps for the three different classes: "background", "cuboid", and "cylinder". Brightness in the output maps represents the probability of individual voxels to belong to the respective classes. For example, white pixels in the second column represent a high probability for this voxel to belong to the background. In Figure 5(b) the brightness of most pixels in the "cylinder" mask is significantly higher than in the "cuboid" mask. This indicates that the U-Net correctly classifies the respective voxels to be part of a cylinder.

While our current implementation focuses on differing between "cuboid"-shaped and "cylinder"-shaped defects, it is relatively straight-forward to adapt to other defect types. To do so, the neural network only needs to be modified with respect to the number of output classes. The training process itself is very much the same, no matter which defects need to be detected. If available, also real annotated data can be used for training. This makes the method quite flexible and adaptable to varying requirements and scenarios.

6. CONCLUSIONS AND FUTURE WORK

We outlined an approach for a highly automated robotic workcell for ultrasonic inspection of complex CFRP parts. Our approach includes a novel path planning algorithm. We use a deep neural network for defect detection and classification of ultrasonic test data of CFRP parts.

In future work we plan to improve the complete workflow by iterative refinement of the different algorithms involved. For coverage planning, we will work with increasingly complex

shapes. With respect to defect detection and classification we will evaluate more scan data to determine the limits when using artificial training data for neural network training.

7. ACKNOWLEDGEMENTS

Work presented in this paper has received funding from the Clean Sky 2 Joint Undertaking (JU) under grant agreement No 831830. The JU receives support from the European Union's Horizon 2020 research and innovation programme and the Clean Sky 2 JU members other than the Union. Work presented in this paper has also received funding by the European Union in cooperation with the State of Upper Austria within the project "Investition in Wachstum und Beschäftigung" (IWB).

8. REFERENCES

[1] M. Okulla, U. Düfert, A. Bulavinov, R. Pinchuk, Fortschrittliche Prüfmethoden zur Prüfung von CFK-Großkomponenten mit komplexer Geometrie, Jahrestagung der Deutschen Gesselschaft für zerstörungsfreie Prüfung, 2017.

[2] E. Galceran and M. Carreras, A survey on coverage path planning for robotics, Robotics and Autonomous Systems, pp. 1258-1276, 2013.

[3] D. Kaljaca and B. A. Vroegindeweij, E. J. van Henten, Coverage trajectory planning for a bush trimming robot arm, J. Field Robotics, vol. 37, pp. 283-308, March 2020.

[4] N. Atkar, H. Choset, A. Rizzi, E. Acar, Exact Cellular Decomposition of Closed Orientable Surfaces Embedded in R3, Proceedings of the 2001 IEEE International Conference on Robotics and Automation, May, 2001.

[5] O. Ronneberger, P. Fischer, and T. Brox, U-Net: Convolutional networks for biomedical image segmenta-tion, International Conference on Medical Image Computing and Computer-Assisted Intervention, pp. 234-241, Springer, 2015.

[6] M. Pedersen, S. Bengtson, R. Gade, N. Madsen, T.B. Moeslund: Camera Calibration for Underwater 3D Reconstruction Based on Ray Tracing Using Snell's Law. CVPR Workshops, pp. 1410-1417, 2018.

[7] G. Paul, N. Kwob, D. Liu: A novel surface segmentation approach for robotic manipulator-based maintenance operation planning, ScienceDirect 2013.

[8] A. Sucan, Mark Moll, Lydia E. Kavraki, The Open Motion Planning Library, IEEE Robotics & Automation Magazine, 19(4):72-82, December 2012.

[9] Ö. Çiçek, A. Abdulkadir, S. Lienkamp, T. Brox, O. Ronneberger: 3D U-Net: Learning Dense Volumetric Segmentation from Sparse Annotation, International Conference on Medical Image Computing and Computer Assisted Intervention (MICCAI), 2016.